Precision measurements of the antiproton-proton elastic scattering cross-section at 90⁰ in the incident momentum range between 3.5 GeV/c and 5.7 GeV/c.

R-704 collaboration

C. Baglin [1], S. Baird [2], G. Bassompierre [1], C. Biino [7], G. Borreani [7], J.C. Brient [1],
J.M. Brom [6], L. Bugge [5], T. Buran [5], J.P. Burq [4], A. Bussière [1], A. Buzzo [3],
R. Cester [7], M. Chemarin [4], M. Chevallier [4], B. Escoubes [6], J. Fay [4], S. Ferroni [3],
V. Gracco [3], J.P. Guillaud [1], E. Kahn-Aronsen [2], K. Kirsebom [5], B. Ille [4], M. Lambert [5],
B. Larsen [5], L. Leistam [2], A. Lundby [2], M. Macri [3], F. Marchetto [7], M. Mattera [3],
E. Menichetti [7], B. Mouëllic [2], N. Pastrone [7], L. Petrillo [8], M.G. Pia [3], J. Poole [2],
M. Poulet [1], A. Pozzo [3], G. Rinaudo [7], A. Santroni [3], M. Severi [8], G. Skjevling [5],
S. Stapnes [5] and B. Stugu [5]

Abstract

The high antiproton-proton luminosity obtained by using a target system consisting of a hydrogen gas-jet crossing a coasting beam of cooled antiprotons circulating in one of the rings of CERN's ISR provides the possibility to measure low cross section reactions with very high precision. We present measurements of the antiproton-proton elastic cross-section at 90⁰ CM at incident momenta between 3.5 GeV/c and 5.7 GeV/c. The precision of these measurements is much higher than previously reported results. The data show that the cross-section of this reaction decreases faster than s^{-12} over this momentum range.

(Submitted to Physics Letters)

[1] LAPP, Annecy, France
[2] CERN, Geneva, Switzerland
[3] INFN and Dipartimento di Fisica dell'Università, Genoa, Italy
[4] IPN, Lyon, France
[5] Physics Department, University of Oslo, Norway
[6] CRN Strasbourg, France
[7] INFN and Istituto di Fisica Superiore dell'Università, Turin, Italy
[8] INFN and Dipartimento di Fisica dell'Università, "La Sapienza" Rome, Italy

1. Introduction.

The experiment R-704 at the CERN ISR used a circulating antiproton beam and a hydrogen gas-jet target to obtain very high antiproton-proton luminosity. Although the experiment was dedicated to the detection of electromagnetic decays of charmonium [1-5], a few runs with a trigger accepting hadrons were performed. The integrated luminosity collected during these runs is sufficient to provide precision data on some processes which were rather poorly measured earlier due to low statistics. Here, we present measurements of the antiproton-proton elastic cross-section at a center of mass angle of 90^0 and incident momenta between 3.5 GeV/c and 5.7 GeV/c.

2. Experimental Apparatus.

The R-704 detector system consisted of two non-magnetic spectrometer arms mounted symmetrically around the interaction region, covering the polar angle from 17^0 to 66^0 in the laboratory frame. Each arm covered an azimuth of 45^0 and consisted of a section designed for charged particle tracking followed by a segmented electromagnetic calorimeter. The first part consisted of scintillation hodoscopes used for triggering on charged particles, a threshold Cherenkov counter for triggering on electrons, and a set of multiwire proportional chambers (MWPCs) for tracking. Each detector arm included two MWPCs, placed at distances of 30 cm and 82.5 cm from the small antiproton-proton interaction region (with a volume of about 1 cm^3). Each chamber contained three wire planes at different orientations. The wire spacing was 2 mm. The calorimeter part consisted of a precalorimeter (a lead/scintillator sandwich of $5X_0$), proportional chambers with analog readout, a scintillator "shower" hodoscope and finally a lead-glass wall ($10X_0$). A system of veto counters surrounded the two detector arms covering a polar angle from 1.7^0 to 77^0 and the full azimuthal angle. The remaining solid angle (polar angles less than 1.7^0 and larger than 77^0) remained uncovered. Small angle elastic scattering events were used for luminosity measurement and monitoring. The recoiling protons were detected with a set of silicon counters mounted at polar angles ranging from 84^0 to 87^0 with respect to the incoming beam. Another measure of the luminosity was deduced from simple coincidence rates in pairs of scintillators. All luminosity monitors were real-time gated.

An extensive description of the apparatus is found in ref. [1].

3. Data Collection and Analysis.

a) Trigger :

The data collected can be grouped in four sets of incident momenta. The momenta and the momentum ranges are the following : 3650±25 MeV/c, 3830±10 MeV/c, 4070±5 MeV/c and 5650±100 MeV/c. The momentum range covered in each of these bins corresponds to the range covered when scanning for charmonium. The trigger was designed to accept events with a single charged particle in each detector arm, and no signal in the veto counters. The charged multiplicity should not be larger than 1 in any of the hodoscope or shower hodoscope planes. In order to be able to correct for losses due to this tight multiplicity requirement, a few runs were performed without any requirements on the hodoscope multiplicity. We refer to [1] for further details on the trigger, but recall here that the definition of a charged particle in a detector arm required a hit in all scintillator planes, including the shower scintillator plane which was situated downstream of 5 radiation lengths (0.3 nuclear collision length) of material. No specific kinematical correlation was required at the trigger level. However, in order to reduce the rate further, events with particles at small angles in both detector arms were rejected. In addition to providing data for this analysis, these "hadron runs" were also used as a tool to study the performance of the detector.

b) Data reduction :

In order to speed up the analysis, the hit pattern in the MWPCs was studied before track reconstruction. Unless contaminated with clusters due to chamber noise or some kind of physical

process (e.g. back-scattering from the calorimeter), one should, for an elastic event, expect just one cluster of hits in each of the six MWPC planes in a detector arm. A mild requirement was imposed in both arms independently; if two or more clusters were found in at least two of the first three MWPC planes, the trigger was rejected. This cut effectively removed multitrack events, hence increasing the speed of the analysis considerably. The loss of good events due to this filter was studied by analysing a few runs twice, once with and once without this filter. It was found that $(6.8\pm2)\%$ of the events were lost due to the filter. The remaining triggers were subjected to track reconstruction. Whenever a combination of tracks with a good vertex reconstruction also satisfied elastic kinematics to within certain cuts in coplanarity and the opening angle, the event was retained (see fig. 1).

c) Final analysis :

The remaining events were subjected to a kinematical fit, using energy and momentum conservation as constraints. Only events with a χ^2/nd of less than 10 were retained (nd is the number of degrees of freedom in the fit). The remaining background was studied in two different ways. First, the distribution of the confidence level deduced from the χ^2 distribution was studied, it is expected to be flat for a sample with only good events. An accumulation of events towards low confidence levels was interpreted as the presence of background (fig 2). A way to check this method was to use a sample of background free $\psi \to e^+e^-$ events [1]. Unfortunately this sample did not contain more than 158 events, but its study suggests that the background is slightly overestimated using this method. This first method was cross-checked by studying a bi-dimensional plot of the coplanarity vs. the difference between the expected and reconstructed polar angle for one of the tracks (see fig. 1). This yielded results compatible with the first method. In conclusion, we adopted the first method, but assigned a systematic error of 4 % to the cross-section calculation due to a possible over-estimate of the background. The background level varied between 10% and 30% depending on the incident momentum.

4. Cross-section calculation.

Only events with $|\cos(\theta^*)| < 0.04$, where θ^* is the centre of mass scattering angle, were considered. Background and correction factors were estimated separately for each energy, and for different trigger conditions. The cross-section is given by :

$$\frac{d\sigma}{d\Omega} = \frac{N - N_B}{2\pi \, \Delta\cos(\theta^*) \, L \, K} \tag{1}$$

where N is the number of events, N_B is the number of background events, $\Delta\cos(\theta^*)$ is the range in the cosine of the scattering angle at which events were collected ($\Delta\cos(\theta^*) = 0.08$), L is the integrated luminosity and K is a correction factor accounting for geometrical acceptance and inefficiencies. The geometrical acceptance was calculated by Monte-Carlo and found to be ranging between 21% and 25%, depending on incident momentum and trigger matrix setting. The correction factor due to the tight trigger multiplicity requirement accepting one and only one hit in each scintillator plane was estimated by studying particularily good event candidates of runs without any condition on the multiplicity. This correction turned out to be rather large; just 47.3 ± 0.5 % of the elastics had a multiplicity of exactly 1 in all of the hodoscope planes. This is explained by the large fraction of protons (or antiprotons) expected to initiate a hadronic shower in one of the precalorimeters, each of a thickness of 0.3 interaction length, hence the charged multiplicity often becomes larger than 1 at the entrance of the shower hodoscope. Another trigger inefficiency is due to the possibility that the charged particles could be stopped altogether before reaching the shower hodoscope. Unfortunately, a correction due to this effect cannot be estimated from our data. However, knowing the mean range of protons of a few GeV/c, one may estimate the loss due to this effect to be about 5% (with a small variation over our energy range). The product of the remaining efficiencies (MWPC filter and reconstruction efficiencies) was typically somewhere between 80% and 85%. The correction factor, K, was estimated on a run to run basis, and was typically somewhere between 0.07 and 0.09. In table 1 we summarize the results.

5. Discussion.

In fig. 3 we show a log-log plot of $d\sigma/dt$ at 90^0 CM versus s, the square of the centre of mass energy. The precision of our data points with respect to previous measurements is clearly visible. A fit of the form s^{-n} has been performed using our four data points, neglecting the systematic errors. The fitted value is $n = 12.3$, but clearly the data do not seem to behave according to a power law of this type. When compared with pp data, it is noted that the $p\bar{p}$ cross-section falls off much faster than the pp cross-section. This contradicts two well known models for elastic scattering, the dimensional counting rule [6], and the constituent interchange model [7], both predicting power law behaviour of the cross-section with the same exponent for both the pp and the $p\bar{p}$ case ($n = 10$ and $n = 12$ respectively). In fig.4 we show the ratio between the pp and the $p\bar{p}$ elastic scattering cross-section at 90^0 as a function of s. Our data confirm the previously noted trend of a change of this ratio over the range of energies for these measurements [8].

6. Conclusions.

We have presented measurements of the antiproton-proton elastic cross-section at 90^0 CM for several incident momenta in the range between 3.6 and 5.7 Gev/c. The precision of these measurements is superior to previously reported measurements from dedicated experiments. The cross-section seems to fall off faster than s^{-12} over this energy range.

Table 1. Summary of results for the measurements of the antiproton-proton elastic scattering cross-section at 90^0 CM.

p	N	L	$d\sigma/d\Omega$	$-t$	$d\sigma/dt$	Relative error(%)	
GeV/c		nb^{-1}	μb/ster	$(GeV/c)^2$	$\mu b/(GeV/c)^2$	stat	syst
3.65	3151	12.04	4.75	2.65	11.20	1.8	10.0
3.83	684	2.16	4.12	2.78	9.29	3.8	10.0
4.07	1577	10.32	2.23	3.03	4.61	2.6	10.0
5.65	107	21.06	0.043	4.50	0.060	19.0	13.0

Figure captions.

Fig.1)
Scatter plot of the coplanarity versus $\Delta(\theta)$ for a sample of triggers. The coplanarity is defined as $\cos(\xi)$, where ξ is the angle between the incoming beam and a vector normal to the plane spanned by the two outgoing particles. $\Delta(\theta)$ is the expected minus reconstructed polar angle in arm 1 of the detector. The small square indicates the limit for accepted events ($|\cos(\xi)| = 0.01$ and $|\Delta\theta| = 15$ mrad). The region between the large and the small square was studied in order to get an estimate of the background.

Fig.2a)
Distribution of the kinematical χ^2 per degree of freedom (χ^2/nd) for the elastic scattering hypothesis. The events are those passing the cuts mentioned in figure 1.

Fig.2b)
Confidence level (c.l.) distribution. The curve is a straight line fit to the distribution between c.l. $= 0.2$ and c.l. $= 1$, and was used to estimate the background level in the sample.

Fig.3)
The $p\bar{p}$ and pp elastic differential cross-sections at 90^0 CM as function of the square of the CM energy, s. Open circles are pp data from [13]. These data fit well to the drawn curve proportional to s^{-9}. The remaining points are $p\bar{p}$ data. Shaded circles from this experiment. Otherwise from [9] (open square), [10] (open triangle), [11] (shaded triangle) and [12] (shaded square). The lower curve is an s^{-n} fit to four data points of this experiment, neglecting systematic errors. One obtains $n = 12.3 \pm 0.2$, but evidently the data do not seem to follow this kind of a power law.

Fig.4)
The ratio between pp and $p\bar{p}$ elastic cross-sections at 90^0 as function of s. The figure is taken from [8] with our data points (shaded circles) added. The pp data used for calculating these ratios for our data points are from [13].

References.

1. R704 Collab., C. Baglin et. al. Nucl. Phys. B286 (1987) 592.
2. R704 Collab., C. Baglin et. al. Phys. Lett. B 171 (1986) 135.
3. R704 Collab., C. Baglin et. al. Phys. Lett. B 172 (1986) 455.
4. R704 Collab., C. Baglin et. al. Phys. Lett. B 187 (1987) 191.
5. R704 Collab., C. Baglin et. al. Phys. Lett. B 195 (1987) 85.
6. S. J. Brodsky and G. Farrar: Phys. Rev. D11 (1975) 1309.
7. J. F. Gunion, S. Brodsky, R. Blankenbecler : Phys. Rev. D8 (1973) 287.
8. P. J. Carlson, K. E. Johansson : Lett. Nuov. Cim. Ser. 2 17 (1976) 379.
9. W. M. Katz et al.: Phys. Rev. Lett. 19 (1967) 265.
10. O. Czyzewski et al.: Phys. Lett. 15 (1965) 188.
11. A. Eide et al.: Nucl. Phys. B60 (1973) 173.
12. T. Buran et al.: Nucl. Phys. B97 (1975) 11.
13. R. Kammerud et al.: Phys. Rev. D4 (1971) 1309.
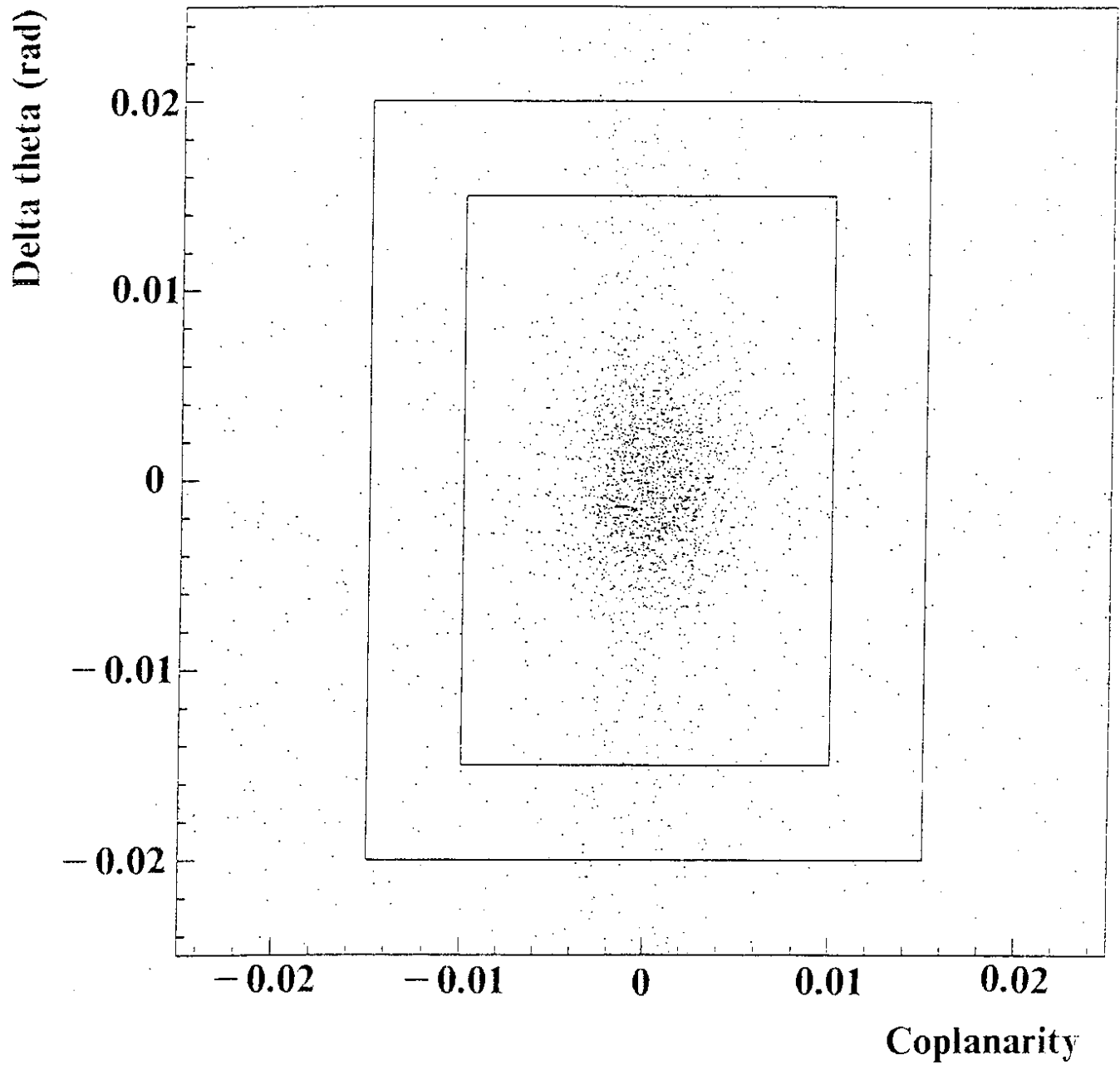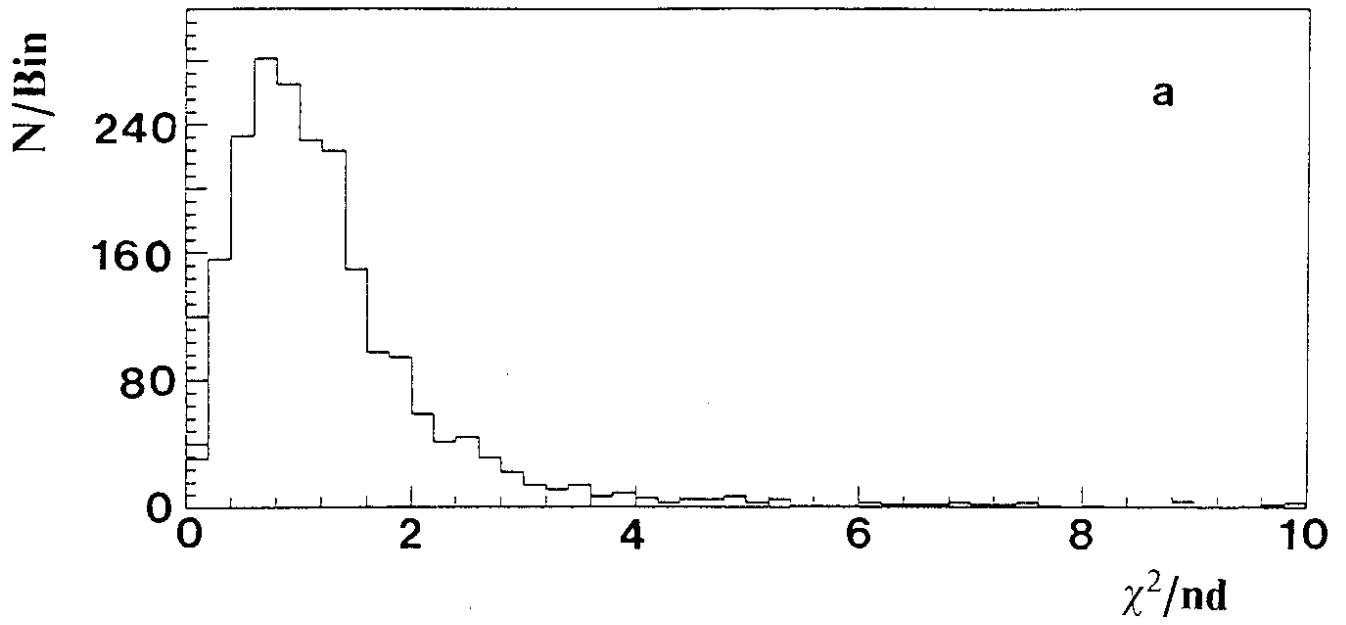
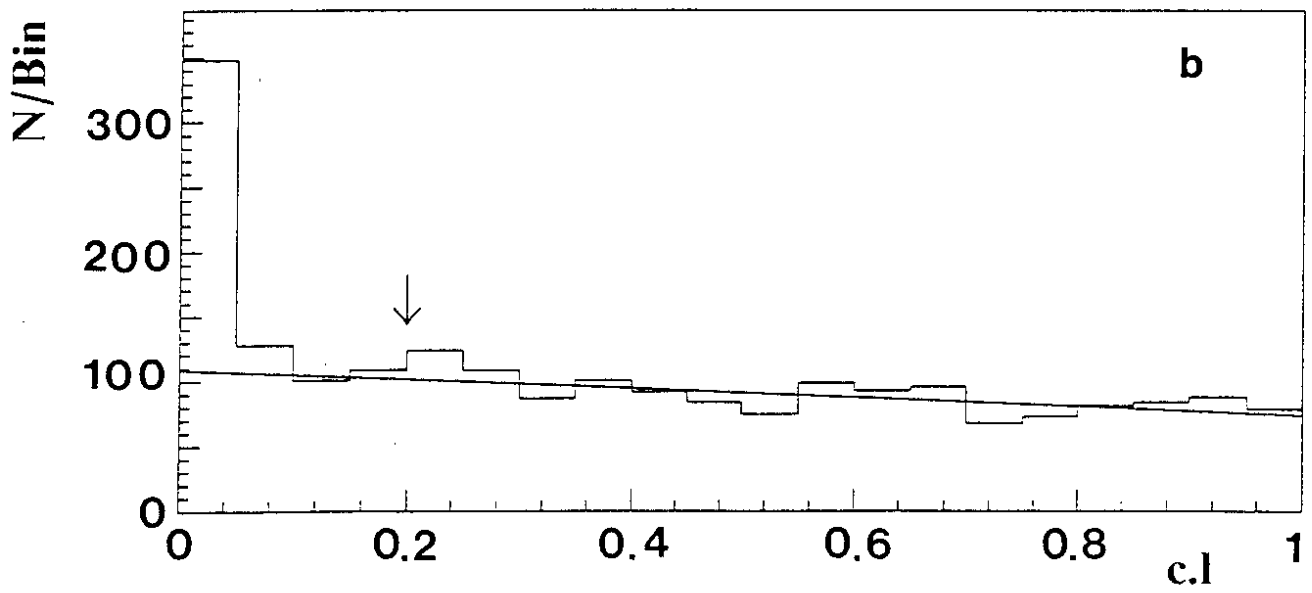# Delta theta vs. coplanarity

Fig. 1

χ^2/nd distribution

a

Confidence level

b

Fig. 2

Cross-sections at 90 degrees

Legend:
- ○ Kammerud et al. (pp)
- ● This experiment
- □ Katz et al.
- △ Czyzewski et al.
- ▲ Eide et al.
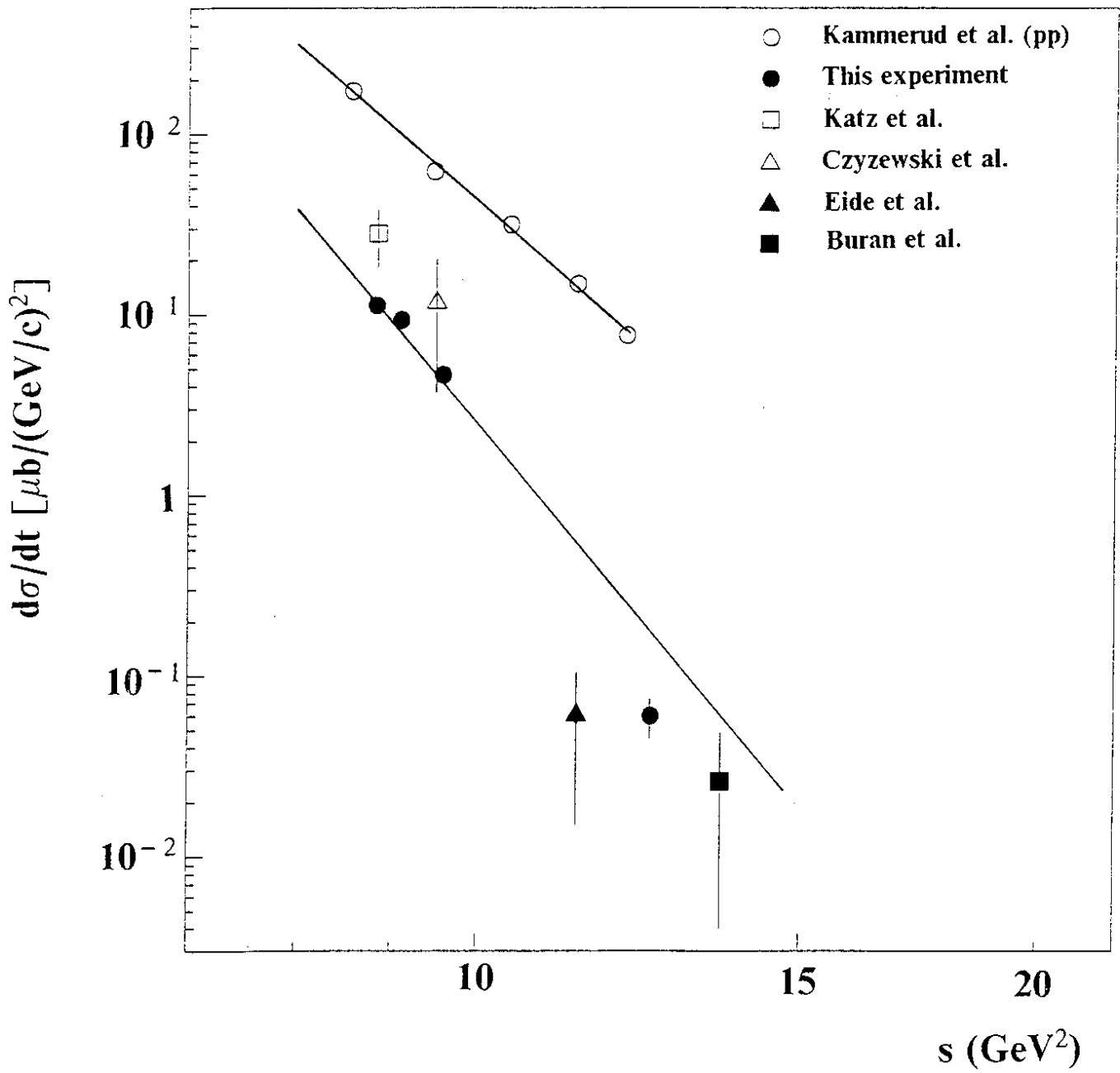- ■ Buran et al.

Y-axis: $d\sigma/dt$ [μb/(GeV/c)^2]

X-axis: s (GeV^2)

Fig. 3

Ratio between cross-sections

Fig. 4